Volumetric Anatomical Parameterizations

****** ****[1,2], ****** ** ******** *********[1], and ****** ***[2] ⋆

[1] **** ** *******, *********, *****
[2] ******** ****** ******, ***** ******* ****, *********** ******** ** *********, *****

Abstract. A coordinate system parameterizing the interior of organs is essential for a systematic localization of injured tissue. If, in addition, same coordinate values are assigned to specific anatomical sites, parameterizations ensure integration of data across different medical image modalities. Harmonic mappings have been extensively used to produce parametric meshes over the surface of anatomical shapes, given their flexibility to set values at specific locations through boundary conditions. However, most of existing implementations restrict to either anatomical surfaces or the depth coordinate with boundary conditions given at sites of limited geometric diversity. In this paper, we present a method for anatomical volumetric parameterization that extends current harmonic parameterizations to the interior anatomy using information provided by the volume medial surface. We have applied our method for parameterizing livers and a brain including the ventricles.

Keywords: Heat equation, Coordinates, Parameterizations

1 Introduction

In the definition of volumetric coordinate systems adapted to the anatomy geometry a radial or depth coordinate is mandatory in a wide range of medical applications covering neuroanatomy [22,16], cardiac modelling [17], and cancer treatment planning [4,15]. Besides they allow integration of multimodal data across subjects provided that the coordinate system assigns equal values to equivalent anatomical sites [7,18,20].

In the context of differential geometry, a parameterization [14] of a given n-dimensional topological manifold is defined by one to one local maps between the manifold and a domain of the n-dimensional Euclidean space. By considering the level curves of the Euclidean space coordinate axis, parameterizations generate regular coordinate meshes on the volume. A main requirement for defining valid coordinate curves from parametric maps is that they need to be smooth (diffeomorphic) functions. Therefore, most methods are based on the harmonic function

⋆ **** ******** *** **** ****** ** *** ******* ******* *************, ******* ******** **************, ************ *** *** ******** ***** *** ***** ********* *** ******* ****** that solves the Laplacian equation with Dirichlet boundary conditions. Dirichlet boundary condition allow setting given coordinate values at some anatomical sites [6]. The coordinates fixed on such sites propagate over the whole domain and, thus, their variation uniquely determines the parametric map. In medical applications, harmonic maps have been used for defining surface coordinates on spherical organs, such as brain sulci [20] and brain internal parts [16]. The potential of harmonic Partial Differential Equations (PDE) for defining coordinates in the whole 3D volume of complex anatomies has been hardly explored. There are two main methodologies for defining volumetric coordinates: volume approximation using basic functions and medial representations.

The performance of basic function approaches is highly dependent on the type of function (B-splines, spherical harmonics, ...) used to approximate volume geometry. Most methods use spherical harmonics and, thus, restrict to volumes of spherical type, like the brain [1]. Although recent works [9] have applied other basic functions (Hermite polynomials) for generating regular meshes over more complex geometries (like the myocardium), they do not provide, indeed, a parametric mapping. Medial representations [2] describe anatomical volumes using the perpendicular (radial) direction to the volume medial surface. Medial representations, such as mreps [11] and more recently continuous mreps [22], have been extensively applied to several medical imaging problems [22,15]. Although medial representations suffice to describe volume geometry, they do not provide parametric coordinates. Besides, they are not well suited for description of the medial branches associated to non-convex shapes. A recent work [21], uses a biharmonic PDE to define a radial coordinate for medial surfaces presenting complex branching topologies. The flexibility of the approach allows the parameterization of anatomies as complex as the myocardium [18]. A main concern is that surface coordinates are given by a discrete triangular mesh of the medial surface and, thus, they might not provide a proper parameterization.

This work contributes to the definition of coordinate systems of anatomical volumes in two aspects. First, we present an extension of the works of [3] to 3D domains using information provided by the volume medial surface. Our implementation directly works on the discrete voxel image domain, handles flexible boundary conditions and generalizes well to complex shapes. Second, we also analyze in deep details the capabilities and limitations of the Laplacian for defining anatomical parameterizations valid for implicit subject registration of multimodal data.

2 Discrete Heat Propagation for Volumetric Anatomical Parameterizations

Heat propagation follows the Partial Differential Equation:

$$\frac{\partial u}{\partial t} - k \Delta u = 0. \tag{1}$$

for $u = u(x, y, z, t)$, k the thermal diffusivity and $\Delta = \partial_{xx} + \partial_{yy} + \partial_{zz}$ the Laplacian operator. Solving the heat equation requires the selection of boundary conditions. Boundary conditions take the form of constraint heat values at specified points (Dirichlet), or constraints fixed value of a partial derivative at the point (Neumann). Dirichlet conditions constrain the values of heat (coordinate values) at some specific anatomical sites, which will be extended by the heat equation to the whole domain. This allows to write generic procedures for the computation of coordinates. Given that different boundary condition imply complete different coordinate mappings, their setting is crucial for getting a suitable parameterization of the anatomy.

Parametric mappings are given by the final steady state of heat. A steady state is a heat distribution reached for infinite time that does not change any more. Therefore, parametric mappings solve the Laplacian:

$$\Delta u = 0 \qquad u_{|\mathcal{A}} = f \tag{2}$$

for $f = f(x, y, z)$ the coordinate values defined at anatomical specific sites $\mathcal{A}$ that have to be extended to the whole anatomical volume. In order to parameterize a rich variety of shapes, the discrete implementation of (2) should handle flexible boundary conditions.

We solve equation (2) by finite differences over the voxel sampling of the image 3D domain. The value of the solution at each voxel will be noted by $u_{i,j,k}$ and its neighboring voxels will be given by its connected neighboring voxels. Using second order central finite differences for all directional derivatives over this grid, the Laplace equation is given by:

$$\begin{gathered}(u_{i+1,j,k} - 2u_{i,j,k} + u_{i-1,j,k}) + \\ +(u_{i,j+1,k} - 2u_{i,j,k} + u_{i,j-1,k}) + (u_{i,j,k+1} - 2u_{i,j,k} + u_{i,j,k-1}) = 0.\end{gathered}$$

By applying the Laplace discrete operator to all image voxels, equation (2) can be written in matrix form as $Au = 0$. The matrix A encodes the neighboring relations between voxels. It is called adjacency matrix and can be computed using algorithm 1.

```
input  : D=Voxels of the anatomical domain.
output: Adj=Adjacency matrix.
Adj← Empty matrix of #D × #D;
for v : Voxels ∈ D do
    for n : Neighbors of v do
        Adj(v, n) ← −1;
    end
    Adj(v, v) ← #Neighbors;
end
```

Algorithm 1: Computation of adjacency matrix for an anatomical domain D

Boundary conditions are introduced by setting the values of u to specific coordinate values at voxels belonging to the anatomical sites $\mathcal{A}$. This reduces the solution to the Laplacian with Dirichlet anatomical conditions to solving a system of equations $Au = b$. The boundary values b can be computed using algorithm 2. The full set of discrete equations with the constrains imposed by the boundary conditions define a system of sparse linear equations that can be solved using standard sparse linear system of equation solving methods such as Jacobi, Gauss-Seidel or Successive Over-Relaxation [12].

input : $\mathcal{A}$=Voxels where boundary apply
input : f=Values of each voxel on $\mathcal{A}$
output: b=b matrix on the equation system
for f_i*: each different value of* f **do**
  for v*: any voxel with boundary value* f_i **do**
    add $-f_i$ to rows of b where $Adj(x, v) = -1$;
  end
end

Algorithm 2: Adjacency matrix computation

Similarly to [3] we parameterize volumes using 3D spherical coordinates (latitude, longitude and radial). Boundary conditions are used to set the range of each parameter, latitude$\in [-\pi, \pi]$, longitude$\in [0, 2\pi]$ and radial$\in [0, 1]$.

2.1 Radial Coordinate

For spherical objects, the radial coordinate can be defined from the heat flowing from the volume center of mass to the external boundary. However, for more complex non-convex shapes, the center of mass may lie outside of the boundary of the object. Inspired by medial representations, we consider the object medial surface the loci from where heat can spread to any part of the domain. Medial surface is the loci of center of maximal spheres bi-tangent to the surface boundary points of the shape [2]. By definition [13], medial surfaces are always located in the center of the object, and thus, are an excellent candidate from where heat can spread to the surface of the object. In order to get medial surfaces that do not requiring pruning, while at the same time allow good reconstruction of the original volume, we have used the method [19].

Let $\mathcal{M}$ be the medial surface and ∂D the anatomical volume boundary. Then, the Dirichlet conditions for defining the radial coordinate are given by:

$$f(x, y, z) = \begin{cases} 1, & \text{for } (x, y, z) \in \mathcal{M} \\ 0, & \text{for } (x, y, z) \in \partial D \end{cases}$$

Boundary voxels are determined by searching voxels of the object that are n-connected to background voxels [10,13]. The definition of boundary conditions is sketched in the liver scheme of fig.1(a) that shows in gray a medial surface of a liver schematic anatomy. Radial coordinate obtained over a true liver volume is shown in fig.1(b). We show an axial and longitudinal cuts with a color mapping encoding radial values.

2.2 Latitudinal Coordinate

Latitude is defined along a curve radially traversing the volume and joining two separated points (poles) of the volume boundary, p_n, p_s. These two voxels are

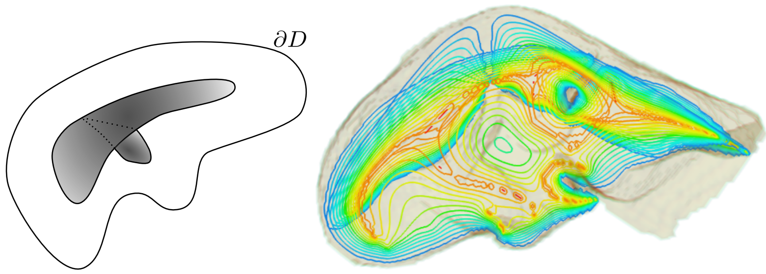

(a) (b)

Fig. 1: Depth coordinate: boundary conditions, (a), values, (b).

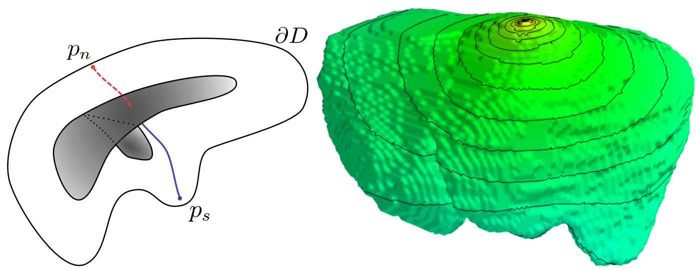

(a) (b)

Fig. 2: Latitude coordinate: boundary conditions, (a), values, (b).

placed on two opposed, maximally separated points on the boundary surface, ∂D. The gradient of the radial map is used to join the two poles p_n and p_s along two curves, γ_{p_n}, γ_{p_s} that go from each pole to the medial surface. The Dirichlet conditions for defining latitude coordinate are given by:

$$f(x,y,z) = \begin{cases} \pi, \text{ for } (x,y,z) \in \gamma_{p_n} \\ -\pi, \text{ for } (x,y,z) \in \gamma_{p_s} \end{cases}$$

The definition of boundary conditions is sketched in the liver scheme of fig.2(a) that shows γ_{p_n} in dashed line and γ_{p_s} in solid one. The latitude is shown in fig.2(b) over the liver surface colored using latitude values and showing its level curves.

2.3 Longitudinal coordinate

Longitude spans from an imaginary surface, meridian surface, than runs from pole to pole defined using the radial and latitude maps. The shortest latitude path over ∂D from p_n to p_s defines the intersection of the longitudinal surface with ∂D. This curve is propagated inwards along the radial direction until it meets the latitude curves γ_{p_n}, γ_{p_s}.

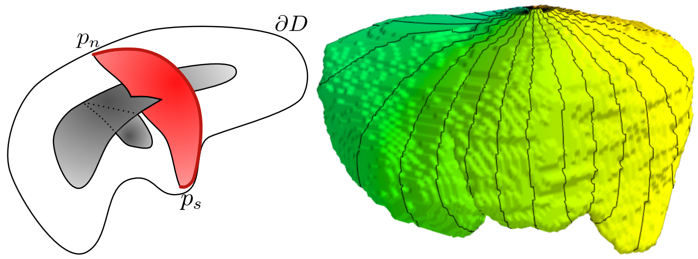

(a) (b)

Fig. 3: Longitude coordinate: boundary conditions, (a), values, (b).

The meridian surface defines the starting of the longitudinal angular parameter. In order to force periodicity, the end of the longitude is assigned to the the neighbouring voxels lying on the meridian left hand-side. Orientation is defined by the sign of the dot product between the normal vector at the meridian surface and the vector from the current meridian voxel to the next. If we note by MS_+ the meridian surface and by MS_- its left replica, then the Dirichlet conditions for the longitude are given by:

$$f(x,y,z) = \begin{cases} 0, \text{ for } (x,y,z) \in MS_+ \\ 2\pi, \text{ for } (x,y,z) \in MS_- \end{cases}$$

The definition of boundary conditions is sketched in the liver scheme of fig.3(a) that shows the meridian surface in red. The longitude is shown in fig.3(b) over the liver surface colored using latitude values and showing its level curves.

3 Discussed Examples

In order to illustrate the flexibility of our volumetric coordinates, we have parameterized livers from Sliver MICCAI challenge [8] and brain volumes from the Center for Morphometric Analysis at Massachusetts General Hospital[3]. Liver lobe distributions introduce a complex convexity in their shape that it is challenging for its 3D parameterization. In the case of the brain, the radial coordinate has been defined from the position of its two ventricles in order to demonstrate the method capability to define flexible coordinates from arbitrary origins.

Figure 4 shows the volumetric coordinate meshes for a representative liver and brain. Left images show the latitude-longitude coordinate mesh over anatomical surface boundaries. Right images show a longitudinal cut with radial-longitude meshes and an axial cut with radial-latitude meshes colored according to depth. For both anatomies, coordinate mappings are smooth functions that define a regular volumetric mesh. Our radial coordinate agrees with the definition required for medial representations and surface coordinates have been perfectly propagated inside volumes parameterizing all depth levels.

[3] http://www.cma.mgh.harvard.edu/ibsr/

For both cases, we observe a rapid decay in the latitude coordinate that produces non-homogeneous meshes. This artifact is intrinsic to using the Laplacian equation for defining surface coordinates and has been reported before [3]. Non-homogeneity is usually solved by a further regularization step over the coordinates computed using the heat equation [3]. Taking into account that solutions to the Laplacian are infinitely smooth such regularization step seems somehow redundant. We attribute the rapid decay to the profile of the fundamental solution [5] to the Laplacian, which is given in terms of the inverse distance to the origin:

$$u(x) = \begin{cases} log(1/r), \ n = 2 \\ \frac{1}{n-2}\frac{1}{r^{n-2}}, n > 2 \end{cases} \tag{3}$$

for r the distance to the origin and n space dimension.

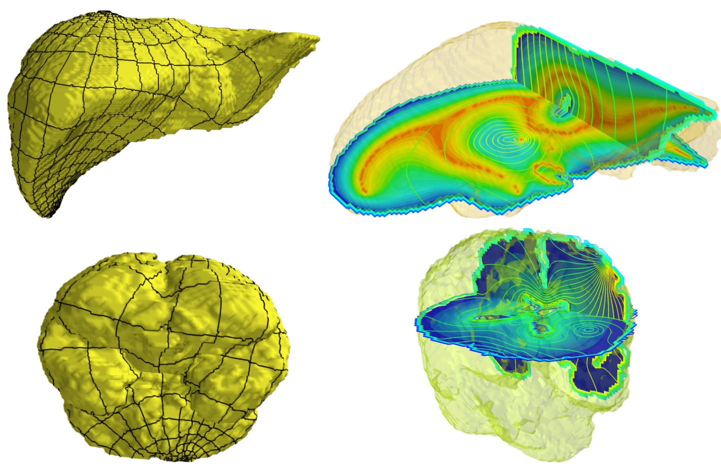

Fig. 4: Liver and brain parameterization.

4 Conclusions

We have presented a flexible method for parameterization of volumetric anatomical shapes, able to provide a parameterization of the depth coordinate regardless of the volume shape. Its applications in medical imaging are promising. The possibility of defining flexible organ centric coordinate systems, will allow analyzing intra-organ structures in a domain-specific framework and comparison of their differences.

We have also identified the sources of mesh artifacts in terms of the Laplacian fundamental solution. This opens the possibility to define a normalization of the coordinates based on a suitable inverse function depending on the fundamental solution for each boundary problem. Such normalization would save further regularization steps and it is our current research line.

References

1. A. Kelemen, G.S., Gerig, G.: Elastic model-based segmentation of 3d neuroradiological data sets. Trans. Med. Imaging 18, 828–839 (1999)
2. Blum, H.: A transformation for extracting descriptors of shape. MIT Press (1967)
3. C. Brechbauhler, G.G., Kabler, O.: Parametrization of closed surfaces for 3-d shape description. Comp. Vis. Imag. Unders 1(61), 154–170 (1995)
4. Crouch, J., Pizer, S., Chaney, E., et al: Automated Finite-Element analysis for deformable registration of prostate images. TMI 26(10), 1379–1390 (2007)
5. Evans., L.: Partial Differential Equations. Berkeley Math. Lect. Notes (1993)
6. Floater, M.S., Hormann, K.: Surface parameterization: a tutorial and survey. In: In Advances in Multiresolution for Geometric Modelling. pp. 157–186 (2005)
7. Gil, D., Garcia-Barnes, J., A. Hernandez, A.: Manifold parametrization of the left ventricle for a statistical modelling of its complete anatomy. In: SPIE. pp. 304–314 (2010)
8. Heimann, T., van Ginneken, B., Styner, M.A., Arzhaeva, Y., Aurich, V.: Comparison and evaluation of methods for liver segmentation from CT datasets. IEEE Trans. Med. Imag. 28(8), 1251–1265 (2009)
9. Lamata, P., Niederer, S., D.Nordsletten, et al: An accurate, fast and robust method to generate patient-specific cubic hermite meshes. MedIMa 15, 801–813 (2011)
10. Malandain, G., Bertrand, G., Ayache, N.: Topological segmentation of discrete surfaces. International Journal of Computer Vision 10(2), 183–197 (1993)
11. Pizer, S., Fletcher, P.e.a.: Deformable M-Reps for 3D medical image segmentation. Int. J. Comp. Vis. 55(2), 85–106 (2003)
12. Press, W.H.: Numerical Recipes Numerical Recipes: The Art of Scientific Computing. Cambridge Univ. Press (2007)
13. Pudney, C.: Distance-ordered homotopic thinning: A skeletonization algorithm for 3D digital images. Comp. Vis. Imag. Underst. 72(2), 404–13 (1998)
14. Spivak, M.: A Comprehensive Introduction to Differential Geometry, vol. 1. Publish or Perish, Inc (1999)
15. Stough, J., Broadhurst, R., Pizer, S., Chaney, E.: Regional appearance in deformable model segmentation 4584, 532–543 (2007)
16. Styner, M., Lieberman, J.A., D., P., Gerig, G.: Boundary and medial shape analysis of the hippocampus in schizophrenia. Medical Image Analysis 8(3), 197–203 (2004)
17. Sun, H., Avants, B., Frangi, A., et al: Cardiac medial modeling and time-course heart wall thickness analysis. In: MICCAI. vol. 5242, pp. 766–773 (2008)
18. Sun, H., Frangi, A., Wang, H., et al: Automatic cardiac mri segmentation using biventricular deformable medial model (2010)
19. Vera, S., Gil, D., Borràs, A., Linguraru, M.G., Ballester, M.A.G.: Geometric steerable medial maps. Machine Visions and Applications (138)
20. Wang, Y., Gu, X., Hayashi, K., Chan, T., et al: Brain surface parameterization using Riemann surface structure (2005)
21. Yushkevich, P.: Continuous medial representation of brain structures using the biharmonic PDE. NeuroImage 45(1), 99–110 (2009)
22. Yushkevich, P., Zhang, H., Simon, T., Gee, J.: Structure-specific statistical mapping of white matter tracts. NeuroImage 41(2), 448–461 (2008)